Ground Support 2023 – J Wesseloo (ed.)
© 2023 Australian Centre for Geomechanics, Perth, ISBN 978-0-6450938-5-8
doi:10.36487/ACG_repo/2325_19

Dynamic impact and static testing of self-drilling dynamic bolt types installed in Normet's urea-silicate injection resin: a new path forward to reducing worker exposure to high-stress ground conditions

A Punkkinen *Normet Canada Ltd, Canada*

G Li *Queen's University, Canada, and Hebei University of Engineering, China*

A Taheri *Queen's University, Canada*

Abstract

In deep mining operations, large deformation of surrounding rock and rockbursts have become unavoidable concerns worldwide, exposing workers to high-stress hazards. In response to these challenges, Normet has developed high-energy dissipation self-drilling dynamic bolt (SDDB®) varieties installed in urea-silicate injection resin. This research evaluates the static and dynamic performance of Normet's fully encapsulated SDDB. To enable a comprehensive evaluation, an innovative test method utilising continuous and split tube configurations was developed to assess the installation of fully encapsulated bolts in both intact surrounding rock and jointed rock mass. The tests included pull tests, shear tests, continuous tube drop tests and split tube drop tests. Static tests provided insights into the yield load, maximum load, failure load, and bolt elongation under tensile and shear stress, while the dynamic tests evaluated the performance of the SDDB during impact and characterised the failure patterns of the bolts. The fully encapsulated Leinster SDDB exhibited a maximum load capacity of 349.8 kN with 80 mm elongation in the pull test. In comparison, the Onaping SDDB withstood a shear load of 282.6 kN and generated a displacement of 27 mm. Furthermore, the Nevada and Nordic coupled SDDB demonstrated a total elongation of 196 mm and withstood an impact load of 271 kN in the drop test. These research findings highlight the exceptional mechanical properties of Normet's SDDB and its efficacy as a dynamic ground support component in high-stress environments.

Keywords: *high-stress, dynamic bolt, mechanical performance, static and dynamic, fully encapsulated*

1 Introduction

Underground hard rock mining plays a critical role in the Canadian mining industry as it supplies essential mineral and metal products that are crucial for meeting societal demands (Akerele 2023; Lhoste et al. 2023). However, the sustainability of this sector is being challenged by the growing depth of mining operations due to the depletion of shallow mineral deposits (Markovic 2022). One of the fundamental disparities between rock conditions at greater depths and near the surface is the substantial increase in ground stress, comprising both in situ and mining-induced stresses. Under high-stress circumstances, it leads to a significant elastic energy in hard rock. This heightened energy accumulation implies that rock failure at depth can release a considerable amount of kinetic energy (Jonak et al. 2020; Kaiser & Cai 2012). Consequently, geotechnical risks, such as rockbursts and large deformations, have become increasingly prevalent in deep mining scenarios (Ranjith et al. 2017). In the past, ground failures and seismic events caused by high ground stress have escalated costs and posed challenges to the support, health, safety and productivity of deep mining projects, rendering numerous sites in Canada and worldwide unfeasible (Morrison 1989; Mazaira & Konicek 2015; Simser 2019).

In the context of deep mining operations, careful consideration of the load applied on the bolts and the installation of bolts are crucial for implementing effective support strategies (He et al. 2012; Campeau &

Gamache 2022). The surrounding rock mass in such operations is characterised by many discontinuities, including major fractures and minor joints. The rockbolt is subjected to a combination of axial tension resulting from the expansion of the surrounding rock mass, and shear forces arising from the displacement of these discontinuities or joints within the rock (Figure 1). Therefore, comprehensive studies on the performance of dynamic bolts need to encompass both static and dynamic loading conditions.

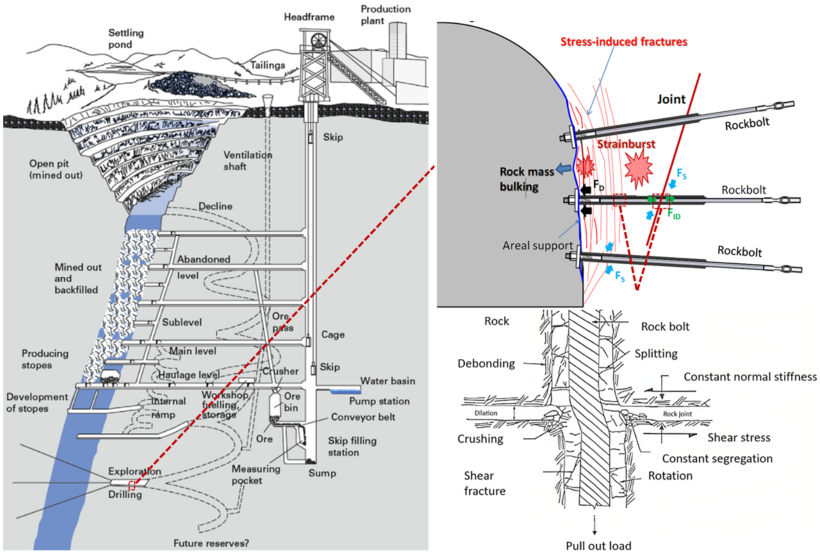

Figure 1 The bolt installation circumstance in deep mining (Manafi et al. 2022; Cai & Kaiser 2022)

The limitations of conventional rebar rockbolts in effectively maintaining stability and mitigating risks in deep mining have been underscored by the uncontrolled deformation of surrounding rock (Kang et al. 2013). Premature bolt failures indicate that the performance of traditional rebar bolts is insufficient to withstand significant rock dilations or dynamic conditions encountered at depth (Ranjith et al. 2017; Wang et al. 2020; Li 2020). Therefore, there is a pressing need for a stronger and more deformable support component in underground excavations subjected to high-stress conditions, aiming to minimise geomechanics-related risks (Saadat et al. 2021).

Cook and Ortlepp initially proposed the concept of yielding support in South Africa's deep gold mines (Cai et al. 2010). Since then, various dynamic bolt designs such as Conebolts, Modified Conebolts, Durabar, Duracable, MCB33, Roofex, Garford bar, D-bolts, He bolts, Dynamic Omega bolts and Dyna Rock bolts have emerged in the market (Bayati et al. 2021; Fuławka et al. 2023; Chen & Li 2015; Kaiser & Moss 2022; Cai 2013; Verma et al. 2021). However, the mechanical performance of existing bolt designs still needs to be improved to better withstand the substantial rock deformations encountered in ultra-deep mining. Furthermore, significant discrepancies exist between the current bolt testing methods and the actual stress conditions experienced in the field, making it challenging to directly apply test results to support design (Taheri et al. 2016a, 2016b; Taheri & Tani 2010). Normet has developed high-energy dissipation self-drilling dynamic bolt varieties (SDDB®) to address the requirements of dynamic support systems. Additionally, the installation of resin-grouted ground support systems in underground mining faces challenges, particularly with remote bolting rigs. Traditional methods involve firing resin cartridges into boreholes using high-pressure air, which can be problematic in fractured ground due to rock fragments and borehole cavitation. The emergence of pumpable urea-silicate injection resins has revolutionised the process, enabling remote application of dynamic ground support with hollow-core bolts. Recent Canadian installations have showcased the efficiency of this approach, surpassing traditional methods in fractured ground conditions and competing with conventional support systems in speed and effectiveness. This research proposes and implements an innovative continuous and split tube testing method to evaluate the behaviour of Normet Canada's urea-silicate injection resin with SDDB under controlled static and dynamic conditions, including pull, shear and drop tests.

2 Testing specimen preparation

2.1 Configuration of SDDB

Normet has developed four R32 types of SDDB bolts, namely the Nevada, the Nordic, the Onaping and the Leinster, to provide design options for mine engineers based on ground conditions and prescribed surface support. The SDDB consists of three sections: the threaded head, the smooth bar and the threaded toe. The configurations of each SDDB type are shown in Figure 2. The ductile smooth bar section is to achieve the desired yield, strength and elongation requirements. The styles are named based on the inside diameter of the bar and the length of each part. For the Nevada bolt (Figure 2a), the outer diameter (OD) of the threaded head is 31.2 mm, the smooth bar has an OD of 32.4 mm and the threaded toe has an OD of 31.2 mm. Similarly, the Nordic bolt (Figure 2b) has respective ODs of 31.2 mm, 32.4 mm and 31.2 mm. The Onaping type bolt (Figure 2c) has an OD of approximately 31 mm. The Leinster type SDDB (Figure 2d) is a modified version of the Onaping type SDDB, where the threaded head is intentionally shortened to allow debonding under load/strain. This modification increases the elongation potential since a longer section of the bar is available for stretching.

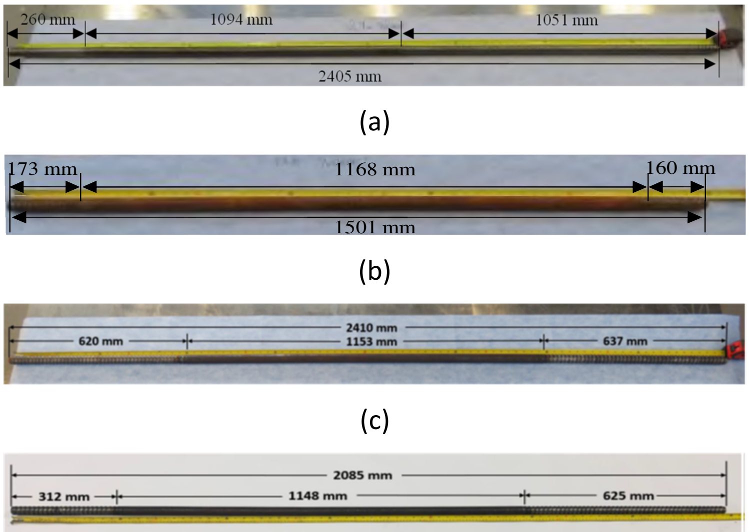

(a) (b) (c) (d)

Figure 2 Configuration of Normet's SDDB types: (a) Nevada; (b) Nordic; (c) Onapling; (d) Leinster

2.2 Test specimen preparation

The tests were completed at CanmetMINING's Ground Control Laboratory in Ottawa, Ontario, Canada. A series of steel tubes with a nominal inside diameter of 47.6 mm and a 12.7 mm-thick wall were prepared for the experiments. These steel tubes were rifled using a modified boring bar. The continuous configuration involved installing the bolt into a steel tube, and the impact or pull was directly applied to the head of the bolt. The split tube configuration involved installing the bolt in a tube made of two joined steel tubes. In this configuration, the impact or pull was not directly applied to the plate at the end of the bolt but rather at a predetermined distance along the tube. In the case of the pull test, two 25.4 mm holes were drilled entirely through the steel tube near its top. These holes provided access to the toe of the bolt and allowed measurement of the bolt end displacement. For the dynamic drop test, two 25.4 mm holes were drilled at the top of the steel tube, and another two were drilled at the halfway point. The top set of holes facilitated the support of the tube within the drop test rig, while the lower set allowed access to the toe of the bolt inside the tube. The tube ends were chamfered to ensure easy assembly into the testing machine and for safety purposes.

2.3 Test specimen installation

The bolts were installed into the steel tubes using resin pumped through the SDDB. This was done by utilising a Normet air-driven resin 1:1 injection pump. A plug was fixed at the end of the tube, extending from the top of the installation tube to below the first 25.4 mm hole, to prevent the insertion of the bolt and the intrusion of grout beyond that point. Additional plugs were fixed into the lower 25.4 mm holes to prevent grout from escaping from the tube during installation. The bolt was inserted into the vertically placed pipe with the plugs at the bottom (Figure 3a) and then filled with injectable resin grout from the collar of the SDDB bolt. A twin-piston pneumatic pump and a nozzle/mixing and head unit were used for injecting the TamPur rockbolt grout (Figures 3b and 3c). A coupler was installed on the threads of the SDDB bolt to attach the nozzle (Figure 3d).

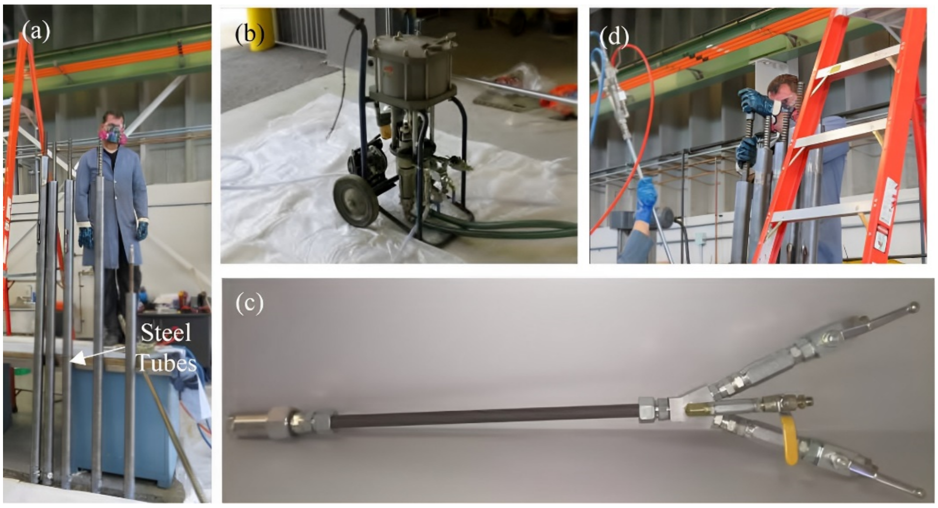

Figure 3 Installation of SDDB: (a) Vertical set-up of the specimens during the installation of the urea-silicate injection resin; (b) The twin-piston pneumatic pump; (c) The nozzle/mixing and head unit; (d) installation of the coupler on the threads of the SDDB

3 Testing procedure

3.1 Set-up of static pull test

For the static pull tests, both continuous and split tube configurations were employed. In the continuous tube test, two hollow hydraulic rams, each with a load capacity of 325 kN, were utilised to exert pressure against a steel plate located approximately 600 mm from the collar of the bolt. A rockbolt plate provided by the experiment set-up was attached to the bolt threads at a distance of about 277 mm (Figure 4a). The pressure applied by the hydraulic rams was measured using an electronic pressure transducer. Two 508 mm stroke potentiometers with a resolution of 0.6 mm were employed to measure displacements.

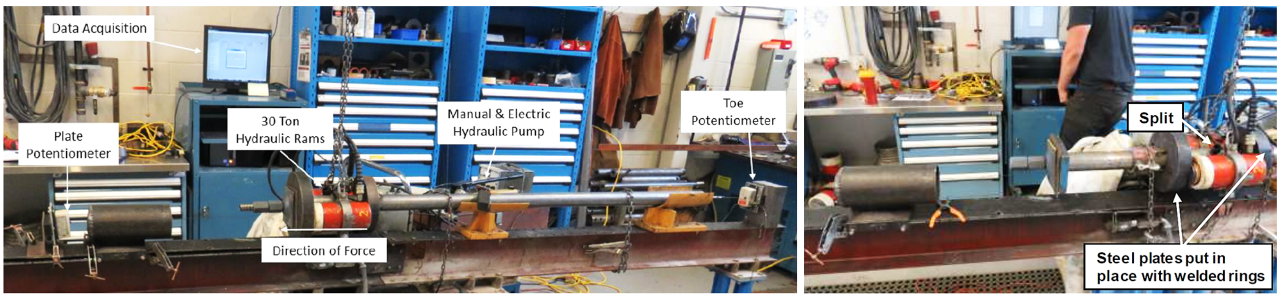

(a) (b)

Figure 4 Set-up of static pull test: (a) Continuous tube test; (b) Split tube test

The split tube test aims to simulate movement across a joint along the installation tube. The set-up for this test is similar to the continuous tube configuration, with the difference that steel plates are positioned using welded rings on the installation tube on each side of the split (Figure 4b). The load rate for both the continuous and split tube configurations is set at 75 kN per minute.

3.2 Set-up of static shear test

The purpose of the static shear tests is to determine the mechanical properties of the transverse sections of the bolts, specifically in either the smooth bar section or the threaded section. These tests were conducted using a shear box and a Super-L120 universal testing machine from Tinius Olsen. Before applying the load, the sample underwent a pre-load to eliminate any slack in the system. Subsequently, a load rate of 3.175 kN/min was applied until failure. The Tinius Olsen press, depicted in Figure 5, illustrates the NEV-8 sample within the shear box.

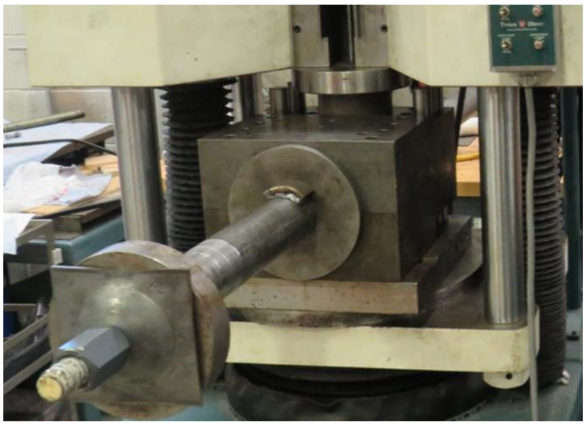

Figure 5 Set-up of the static shear test

3.3 Set-up of dynamic impact drop test

The dynamic performance of the SDDB was evaluated using both continuous and split tube configurations. In the continuous tube configuration, the rockbolt was installed in one tube while leaving the plate anchor outside of the tube. This set-up aimed to simulate the impact directly on the bolt plate when the plate anchor is not encased in resin. The split tube configuration involved impacting the tube further up along its length at a predetermined distance from the plate. This configuration is depicted in Figure 6, illustrating the positioning of the impact in the split tube set-up.

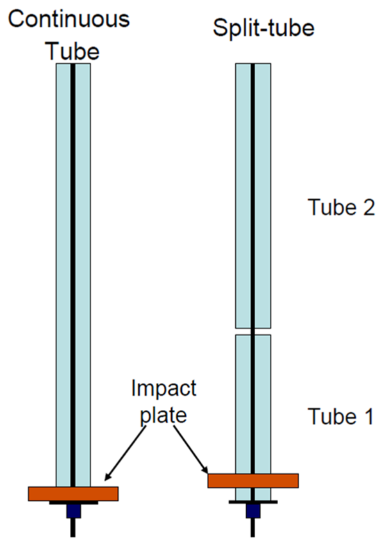

Figure 6 Schematics of the continuous and split tube testing configurations for the dynamic tests

The energy input in the testing system is regulated by adjusting the size of the drop mass and the specified height for the test. The overall set-up of the testing rig, along with detailed views of the top and bottom test assemblies, is illustrated in Figure 7.

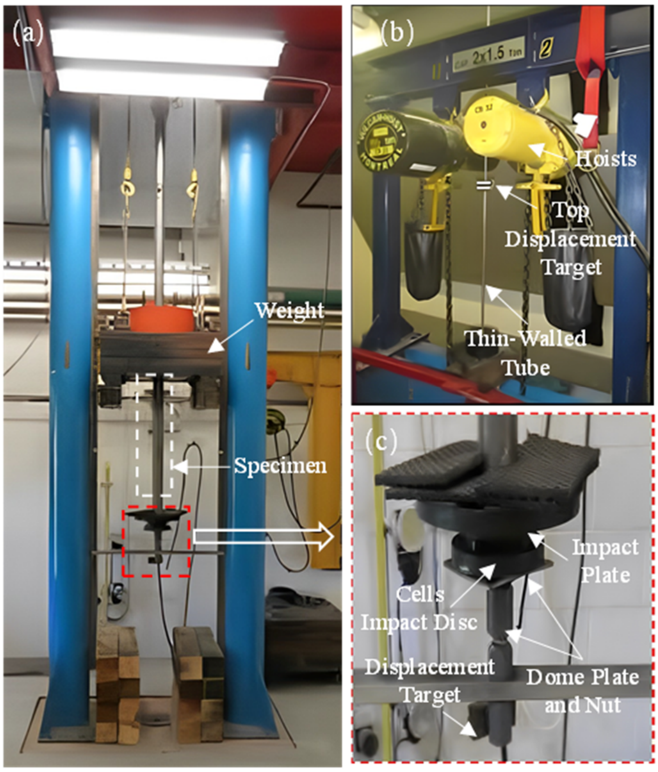

Figure 7 Details of the dynamic testing rig including instrumentation-continuous configuration: (a) General view; (b) Top view; (c) Bottom view

To conduct the test, the installation tube containing the test specimen is inserted through the centre of the magnet and steel plates (Figure 7a). The top end of the installation tube is then connected to a larger tube that is securely fixed to the top of the testing rig. Once the mass is in the holding position, a load cell equipped with a 12 mm-thick impact plate is installed at the lower end of the bolt. Additionally, a rockbolt dome plate and a dome nut are utilised to complete the assembly (Figure 7c). A target is placed to measure the displacement of the lower end of the bolt, specifically on the remaining threaded section. Displacements during the test are accurately measured using line-scan cameras.

4 Results

4.1 Pull test result

One SDDB from the Onaping type (ON-03), one SDDB from the Leinster type (ON-09) and one SDDB from the Nevada type (NEV-1) were subjected to continuous tube pull tests. One SDDB from the Onaping type (ON-11) and one SDDB from the Nevada type (NEV-7) were tested in split tube configuration under tensile load. Furthermore, to validate the structural integrity of the combined SDDB configuration and ensure that the coupler is not the failure point, a Nordic type SDDB was installed in split tube configuration and coupled with a 1-meter threaded section from a Nevada SDDB using a coupler (NEV-7/NOR-4). Hence, the mechanical properties exhibited by the NEV-7/NOR-4 specimen essentially pertain to the Nordic type SDDB. The test results are summarised in Table 1.

Table 1 Pull test results

Specimen ID	ON-03	ON-09	ON-11	NEV-1	NEV-6	NEV-7/NOR-4
Bolt Type	Onaping	Leinster	Onaping	Nevada	Nevada	Nordic
Configuration	Continuous	Continuous	Split	Continuous	Split	Split
Initial bolt length (mm)	2,409	2,085	2,415	2,410	2,413	2,556
Final bolt length (mm)	2,419	2,165	2,511	2,522	2,533	2,625
Elongation (mm)	10	80	96	112	120	69
Yield load (kN)	223.8	255.9	260.4	200.7	186.5	243.4
Maximum load (kN)	355	349.8	353	275.1	256.2	355.5
Failure load (kN)	348.6	349.8	328.8	246.4	227.3	N/A
Plate displacement (mm)	N/A	0	0	117.3	137.5	230.3
Toe displacement (mm)	N/A	0	0	0.4	1.3	126
Elongation (mm)	N/A	83.94	97.13	116.9	136.2	104.3
Failed position past beginning of threads	204 mm	135 mm	790 mm	1,154 mm	757 mm	826 mm

In the pull tests, the ON-03 SDDB sample, which belonged to the Onaping type, achieved the highest maximum load of 355 kN with an elongation of 10 mm. The low elongation value can be attributed to the bonded R32 anchoring within the collar section of the sample. This anchoring prevented the sample from debonding from the surrounding resin, resulting in the force being trapped between the collar and the nut. The failure profile of ON-03 is shown in Figure 8a, where the Normet D17 dome plate completely collapsed during the test.

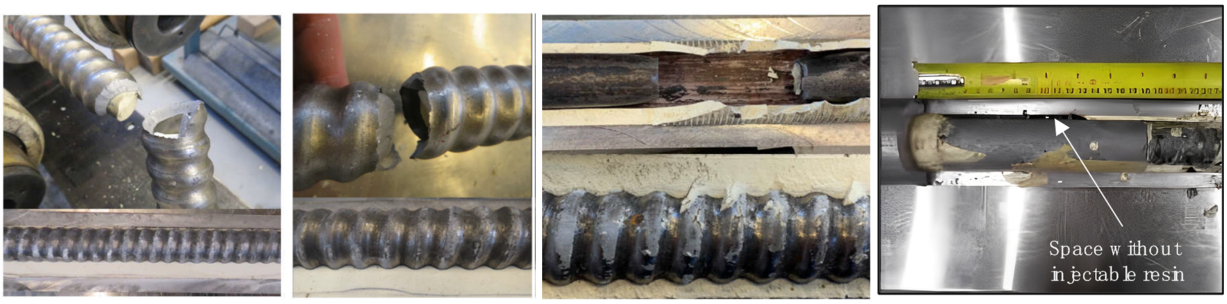

(a) (b) (c) (d)

Figure 8 Failure profile of SDDB in the pull test: (a) ON-03; (b) ON-09; (c) ON-11; (d) NEV-7/NOR-4

The ON-09 sample, which was a Leinster type SDDB, had no anchoring inside the collar section. As a result, the bolt debonded from the resin early in the test, as shown in Figure 8b. The shorter length of threads at the collar section contributed to the early debonding. The ON-09 sample failed 135 mm past the beginning of the threaded section after reaching maximum load of 349.8 kN, as depicted in Figure 9. The ON-11 sample reached a maximum load of 353 kN and experienced an elongation of 97.13 mm before failure (Figure 8c).

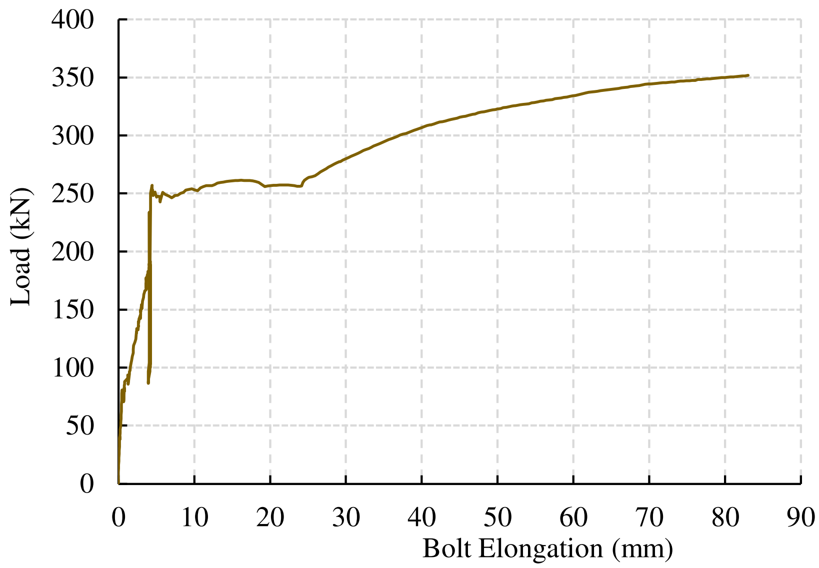

Figure 9 Load versus bolt elongation curve of ON-09 Leinster SDDB in continuous tube pull test

In the static pull tests, the SDDB specimens NEV-1 in continuous configuration and NEV-6 in split tube configuration were broken at distances of 1154 mm and 757 mm, respectively, from the beginning of the threads. The NEV-7/NOR-4 sample experienced sliding during the test, resulting in an elongation of 69 mm. It was broken at the smooth part of SDDB, and the coupler section between the two types of SDDB with stood the tensile as shown in figure 8d. It can be noticed that there is a space without injectable resin between the coupler and the steel tube. The absence of injectable resin reduced the friction force between the coupler and the steel tube, which could explain the sliding of the specimen.

4.2 Shear test result

Three Onaping SDDB, two Nevada SDDB and one Nordic SDDB were subjected to static shear tests to determine their yield and failure loads. The results of these tests are presented in Table 2.

Table 2 Shear test results

Specimen ID	ON-04	ON-12	ON-13	NEV-9	NEV-8	NOR-5
Bolt type	Onaping	Onaping	Onaping	Nevada	Nevada	Nordic
Configuration	Direct shear, the hardened resin in the core	Shear on bolt grouted inside of steel tube	Direct shear, nude bar with no resin	On thread	On bar	On bar
Initial bolt length (mm)	2,412	2,408	2,410	2,395	2,400	1,501
Final bolt length (mm)	2,415	2,411	2,415	2,420	2,420	1,515
Elongation (mm)	3	3	5	25	20	14
Yield load (kN)	75.7	103.8	75.6	76.0	65.4	82.2
Maximum load (kN)	214.6	282.6	206.6	196.5	224.2	259.7
Failure load (kN)	198.2	209.8	182.4	131.3	203.6	166.7
Displacement (mm)	12.4	27	13.2	27.3	31.1	29.0

Figure 10 shows the shear load versus displacement curves of all samples obtained from the shear test. ON-13 was tested without any resin, inside or outside, and reached a maximum load of 207 kN with a yield load of 75.6 kN. ON-04 was installed into a steel tube and then removed so there was hardened resin inside the SDDB's interior. This specimen reached a maximum load of 215 kN with a yield load of 75.7 kN. ON-12 was installed into a split tube configuration and tested as a fully grouted element. This specimen reached a maximum load of 283 kN with a yield load of 104 kN. The higher yield load may be attributed to the compression of the resin in the steel tube. The maximum shear loads obtained for the SDDB specimens were 196.5 kN for NEV-9, 224.2 kN for NEV-8 and 259.7 kN for NOR-5.

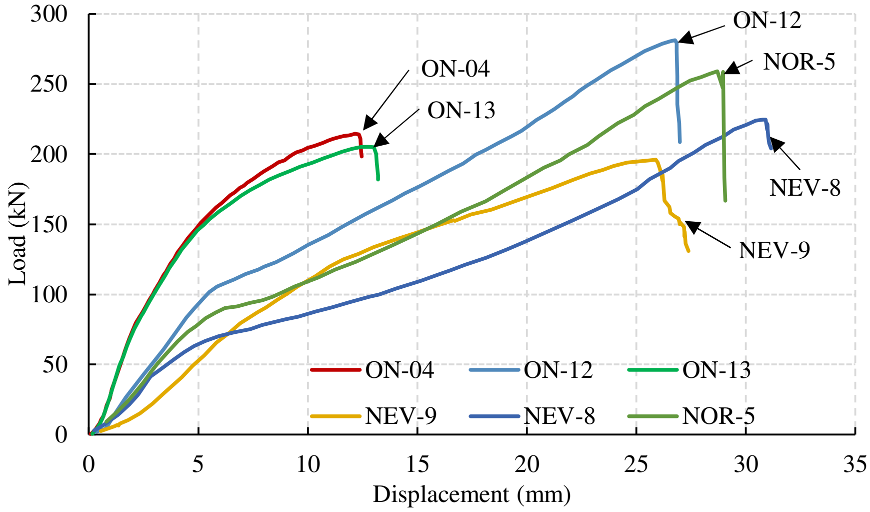

Figure 10 Load versus displacement curve of ON-13 Onaping SDDB in the shear test

In Figure 11d, which represents the shear test conducted on the bar section, it can be observed that the urea-silicate injection resin has been ground and cracked on the opposite side of the shear. The yield load range falls between 65.4 kN and 82.2 kN. It is important to note that the yield point curve for shearing the threaded section is less pronounced compared to shearing the bar section.

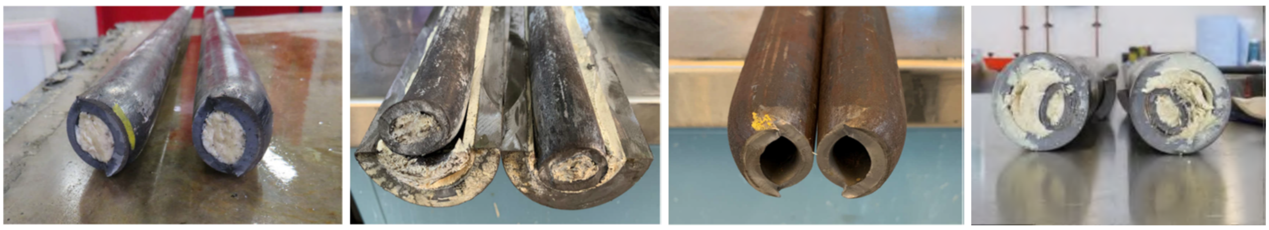

(a) (b) (c) (d)

Figure 11 Failure profile of SDDB in the shear test: (a) ON-04; (b) ON-12; (c) ON-13; (d) NEV-8 and NOR-5

4.3 Dynamic impact test result

4.3.1 Continuous drop tests

Thirteen SDDB were subjected to dynamic drop testing in both continuous and split tube configurations. The test results for the Onaping and Leinster SDDB in the continuous tube configuration are presented in Table 3.

Table 3 Onaping and Leinster SDDB drop test results in continuous tube configuration

Specimen ID	ON-02	ON-15				ON-16			ON-17	
Bolt type	Onaping	Leinster				Leinster			Leinster	
Drop no.	1	1	2	3	4	1	2	3	1	2
Drop mass (kg)	1,338.1	1,338.1				1,783.6			2,006.4	
Drop height (mm)	1,496	1,496				1,430			1,497	
Input energy (kJ)	19.69	19.69				25.02			29.52	
Bolt length before (mm)	1,156	1,151				1,132			1,140	
Bolt length after (mm)	1180.3	1192.4	1244.2	1291.4	1311.0	1199.9	1262.2	1333.5	1218.7	1308.7
Elongation per Drop (mm)	24.3	41.4	51.8	47.2	19.6	67.92	62.26	71.316	78.66	90.06
Strain, per drop (%)	2.1%	3.6%	4.5%	4.1%	1.7%	6.0%	5.5%	6.3%	6.9%	7.9%
Cumulative strain (%)	2.1%	3.6%	8.1%	12.2%	13.9%	6.0%	11.5%	17.8%	6.9%	14.8%
First peak plate load (kN)	423.0	373.0	341.7	373.0	345.8	400.3	359.6	379.0	361.4	380.6

Among the SDDB samples tested in continuous tube drop tests, only ON-02 failed to withstand the first impact. This sample was an Onaping type SDDB with 295 mm of R32 collar anchors bonded. The bolt experienced a strain of 2.1% and stretched by 10 mm before failing at a distance of 201 mm from the beginning of the threads (Figure 12a). Regarding ON-15, its sliding during the fourth impact can be attributed to equipment failure. The rifling on the ON-15 sample was observed to be shallower compared to the other samples. However, the rockbolt itself did not slide within the resin (Figure 12b). The cumulative strains before failure for ON-15, ON-16 and ON-17 were measured as 13.9%, 17.4%, and 14.8%, respectively. ON-16 failed at a distance of 484 mm from the beginning of the threads, while ON-17 failed at a distance of 1,333 mm from the beginning of the threads (Figures 12c and 12 d).

(a) (b) (c) (d)

Figure 12 Failure profile of Onaping and Leinster SDDB after continuous drop test: (a) ON-02; (b) ON-15; (c) ON-16; (d) ON-17

The test results for Nevada and Nordic SDDB samples are presented in Table 4. Only the NOR-1 sample experienced sliding during the second, third and fourth impacts. This sliding behaviour can be attributed to both the weak bond strength and short thread length. With only 1mm of plastic steel stretch after the initial drop, the bolt plowed through the resin from the toe location typical to cone bolt behaviour. In the case of the Nevada SDDB bolt, the plate section was longer and three nuts were used to secure the plate. It was observed that the displacement of the toe section and the plate section were very close after each impact.

Table 4 Nevada and Nordic SDDB drop test results on continuous tube configuration

Specimen ID	NOR-1				NEV-5		
Drop no.	1	2	3	4	1	2	3
Drop mass (kg)	1,338.1				1,338.1		
Drop height (mm)	1.45				1.45		
Input energy (kJ)	19.03				19.01		
Bolt length before (mm)	1,501				2,410		
Bolt length after (mm)	1,584				2,560		
Total elongation (mm)	83				150		
Plate displacement (mm)	42	146	199	193	56	60	N/A
Top displacement (mm)	2	146	198	193	2	1	0
Plastic steel stretch (mm)	40	0	1	0	54	59	-
Plate peak load (kN)	226.1	307.3	204.4	176.2	187.7	279.2	N/A
Plate avg. load (kN)	269.2	115.2	98.9	96.5	228.1	278.6	283.4

Taking NOR-1 as an example, Figure 13 depicts the typical load and displacement versus time curves obtained from the dynamic drop test conducted in the continuous tube configuration. The peak loads recorded for the first impact are 226.1 kN (NOR-1) and 187.7 kN (NEV-5), respectively. These values represent the maximum loads experienced during the impact event.

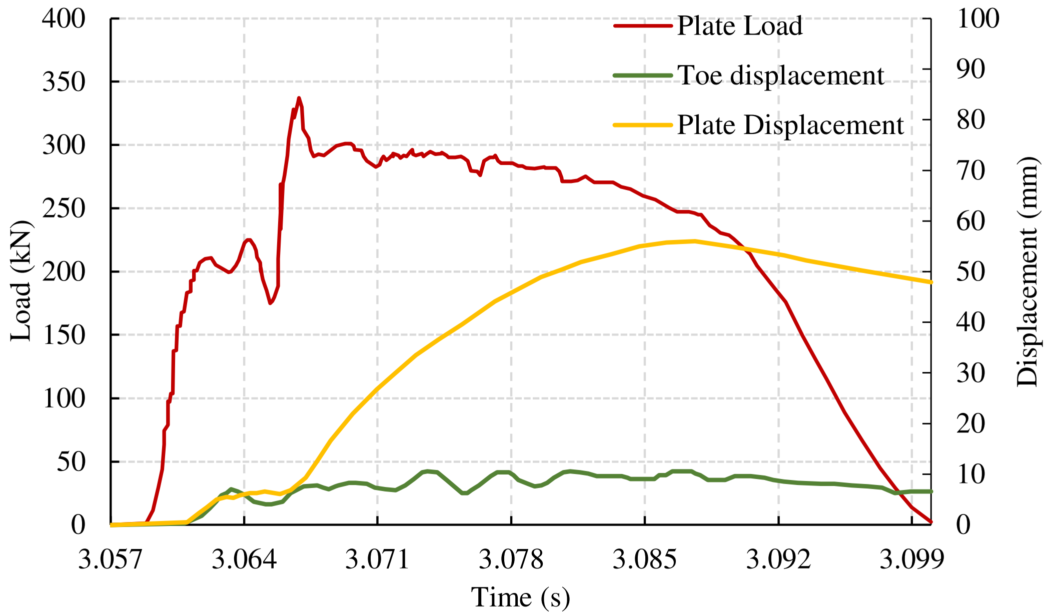

Figure 13 Load and displacement versus time curves of NEV-1 SDDB obtained from dynamic drop test in continuous tube configuration

4.3.2 *Split tube drop tests*

All of the SDDB specimens in split tube configuration successfully withstood the first impact during the drop tests. The results for Onaping and Leinster SDDB are presented in Table 5. However, the ON-08 SDDB was intentionally removed from the dynamic apparatus to prevent equipment failure with an additional drop. The cumulative strain values for ON-05, ON-06, ON-07 and ON-08 were recorded as 20.4%, 18.9%, 19.0% and 12.0%, respectively. Figure 14 displays the failure profiles of the Onaping and Leinster SDDB specimens after the drop tests in split tube configuration.

Table 5 Onaping and Leinster SDDB drop test results in split tube configuration

Specimen ID	ON-05			ON-06		ON-07		ON-08
Drop no.	1	2	3	1	2	1	2	1
Drop mass (kg)	2,006.4			2,451.9		2,674.6		2,897.4
Drop height (mm)	1,496			1,499		1,498		1,755
Input energy (kJ)	29.5			36.1		39.4		50.0
Bolt length before (mm)	1,146			1,144		1,153		1,145
Bolt length after (mm)	1230.8	1307.6	1379.8	1249.2	1360.2	1270.6	1372.1	1282.4
Total elongation (mm)	85.2	76.7	72.3	105.5	110.9	117.7	101.1	137.3
Strain per drop (%)	7.4%	6.7%	6.3%	9.2%	9.7%	10.2%	8.8%	12.0%
Cumulative strain (%)	7.4%	14.1%	20.4%	9.2%	18.9%	10.2%	19.0%	12.0%
First peak plate load (kN)	153.9	127.3	134.1	49.0	60.2	66.8	71.9	108.6

(a) (b) (c) (d)

Figure 14 Failure profile of Onaping and Leinster SDDB after split drop tests: (a) ON-05; (b) ON-06; (c) ON-07; (d) ON-08

The load and displacement versus time curves for NEV-2 are shown in Figure 15. The peak impact/plate load recorded during the first impact was 274 kN and 201.4 kN. Similarly, the peak impact/plate load for the dynamic test of NEV-4/NOR-3 is 273.8 kN and 186.6 kN respectively (not shown). The dynamic drop test results of Nevada and Nordic SDDB in the split tube configuration are presented in Table 6.

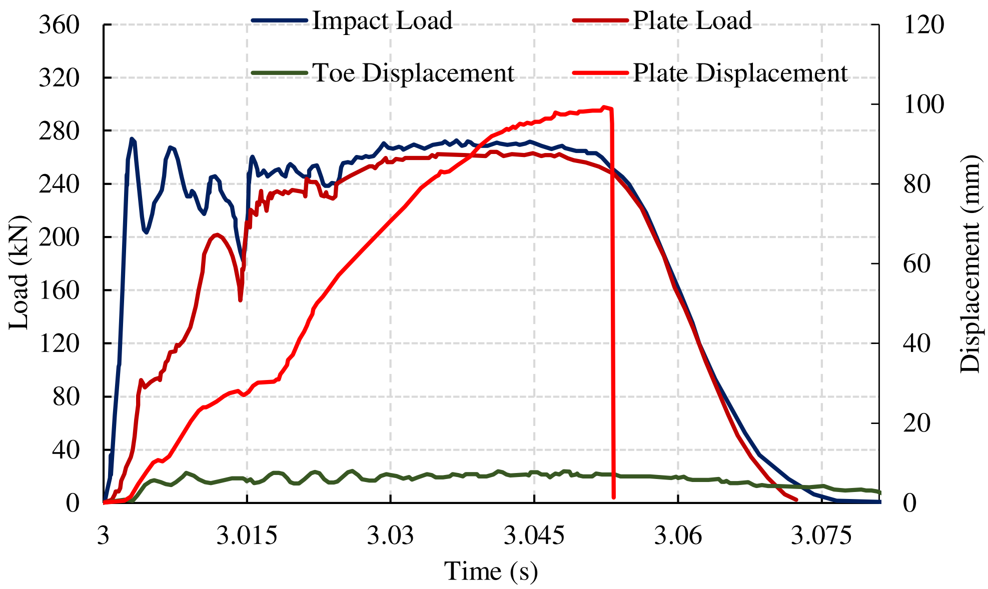

Figure 15 Load and displacement versus time curves of NEV-2 SDDB obtained from dynamic drop test in split tube configuration

Table 6 Nevada and Nordic SDDB drop test results on split tube configuration

Specimen ID	**NEV-2**		**NEV-3/NOR-2/D20 Plate**			**NEV-4/NOR-3**		
Drop no.	1	2	1	2	3	1	2	3
Drop mass (kg)	2,006.35		2,006.35			2,006.35		
Drop height (mm)	1.52		1.52			1.52		
Input energy (kJ)	29.89		29.89			29.89		
Bolt length before (mm)	2,411		2,556			2,550		
Bolt length after (mm)	2,601		2,750			2,746		
Total elongation (mm)	190		194			196		
Plate displacement (mm)	85	N/A	67	83	N/A	77	86	N/A
Top displacement (mm)	2	0	2	1	0	2	1	0
Plastic steel stretch (mm)	83	N/A	65	82	N/A	75	85	N/A
Plate peak load (kN)	201.4	N/A	189.2	340	N/A	186.6	N/A	N/A
Plate avg. load (kN)	244	278.2	267.2	345.1	346.4	271	329.2	329

4.4 Adaptivity of SDDB

In synopsis, the Nevada SDDB design presents early elongation, thereby resulting in lower yield and ultimate strength. In contrast, the Onaping SDDB boasts elevated yield and ultimate strength. The threaded segment of the SDDB within the fractured zone extending beyond the tunnel surface complements surface reinforcement. In contrast, the smooth bar design situated within the unblemished rock interior yields substantial elongation, serving as a dynamic support conduit.

Three select inner hole diameters are provided to achieve the lower-higher yield and ultimate strengths. The Nevada, Nordic and Onaping/Leinster, each with decreasing diameter correspond to increased wall thickness of the dowel and resultant higher strengths. By virtue of its expansive elongation capabilities and formidable resistance attributes, and in tandem with its customisable configuration, Normet's SDDB emerges as an apt choice across a spectrum of underground support scenarios, particularly in challenging contexts such as fractured host rock, heightened ground stress and rockburst-prone areas. The pronounced pre-yielding resistance of the SDDB mitigates the deformation of the encompassing rock. Furthermore, the significant yield deformation inherent in the smooth section dissipates stress concentration, furnishing robust support resistance that effectively curtails the expansion of the surrounding rock under both static and dynamic loading.

The pronounced pre-yielding resistance of the SDDB mitigates the deformation of the encompassing rock. Furthermore, the significant yield deformation inherent in the smooth section dissipates stress concentration, furnishing robust support resistance that effectively curtails the expansion of the surrounding rock under both static and dynamic loading.

The ground control engineer wields the authority to fine-tune essential design parameters encompassing bar length, thread arrangement and smooth section attributes, aligning them meticulously with the specific imperatives of the mining operation. Additionally, the installation procedure may encompass a two-pass protocol entailing the insertion of the bolt within a pre-drilled borehole. In instances where fractured ground conditions are encountered, the integration of a 41-mm sacrificial bit emerges as a prudent strategy. This technique entails drilling the hole while retaining the sacrificial bit in situ, subsequently allowing it to remain within the hole as the bolt is injected using pumpable resin. This method engenders resilient support even in the face of formidable geological challenges.

5 Conclusion

This research involved conducting laboratory mechanical tests on Normet's Onaping, Leinster, Nevada and Nordic types of SDDB to evaluate their static and dynamic performance. A novel testing approach was developed using continuous and split tube configurations to evaluate the installation of fully encapsulated bolts in intact rock and jointed rock masses. Following are the key findings from this research:

Static pull tests yielded the following results: The Onaping SDDB reached a peak load of 355 kN with 10 mm elongation in continuous tube testing. In split tube testing, it achieved a peak load of 353 kN with 97.1 mm elongation. The Leinster SDDB reached a peak load of 350 kN with 83.9 mm elongation. The Nevada SDDB achieved peak tension loads of 275.1 kN (continuous tube), 256.2 kN (split tube). The Nordic SDDB achieved 355.5 kN (Nevada/Nordic coupled sample in the split tube).

Shear tests showed that the Onaping SDDB reached a peak load of 282.6 kN with 27.0 mm displacement. Nevada SDDB's grouted threaded section had a maximum shear load of 196.5 kN with 27.3 mm displacement. Smooth sections of Nevada and Nordic SDDB withstood loads of 224.2 kN and 259.7 kN, respectively.

In the continuous drop test, Leinster, Nevada and Nevada/Nordic SDDB specimens survived the first impact. The Leinster SDDB had peak loads ranging from 361.4 kN to 400.3 kN, with an average strain of 5.5%. Onaping's SDDB failed on the first drop, reaching a peak load of 423 kN with 2.1% strain. Nordic and Nevada SDDB withstood average plate impact loads of 269.2 kN and 228.1 kN, respectively.

Dynamic drop tests in split tube configuration showed all Onaping SDDB withstanding the first impact. ON-08 had only one drop at 50 kJ. The average cumulative strains for the three failed specimens were 19.4%. The Nordic SDDB endured an average plate impact load of 244 kN. Nevada/Nordic coupled SDDB sustained an average plate load of 267.7 kN with 196 mm elongation.

Reference

Akerele, G 2023, *Bench-scale SIR-600 Ion-exchange Column and Cl2 Regeneration for Ammonia Removal from a Simulated Mining Wastewater*, PhD thesis, University of Ottawa, Ottawa.

Bayati, M, Taheri, A, Rasouli, V & Saadat, M 2021, 'A numerical approach to simulate stresses around tunnels in swelling rocks', *Journal of GeoEngineering*, vol. 16, no. 1, pp. 015–022.

Cai, M, Champaigne, D & Kaiser, PK 2010, 'Development of a fully debonded cone bolt for rockburst support', in M Van Sint Jan & Y Potvin (eds), *Deep Mining 2010: Proceedings of the Fifth International Seminar on Deep and High Stress Mining*, Australian Centre for Geomechanics, Perth, pp. 329–342, https://doi.org/10.36487/ACG_repo/1074_24

Cai, M & Kaiser, P, K 2022, 'Selecting the right rockbolts for burst-prone drifts', Proceedings of RaSim10, Society for Mining & Metallurgy, Engelwood, pp. 1–13.

Cai, M 2013, 'Principles of rock support in burst-prone ground', *Tunnelling and Underground Space Technology*, vol. 36, pp. 46–56.

Campeau, LP & Gamache, M 2022, 'Short-and medium-term optimization of underground mine planning using constraint programming', *Constraints*, vol. 27, no. 4, pp. 414–431.

Chen, Y & Li, CC 2015, 'Performance of fully encapsulated rebar bolts and D-bolts under combined pull-and-shear loading', *Tunnelling and Underground Space Technology*, vol. 45, pp. 99–106.

Fuławka, K, Witold, P, Marcin, S, Piotr, M, Bogumiła, P M, Philipp, H, ... Michael, N 2023, 'Prototype of instrumented rock bolt for continuous monitoring of roof fall hazard in deep underground mines', *Sensors*, vol. 23, no. 1, pp. 154.

He, M, Xia, H, Jia, X, Gong, W, Zhao, F, ... Liang, K 2012, 'Studies on classification, criteria and control of rockbursts', *Journal of Rock Mechanics and Geotechnical Engineering*, vol. 4, no. 2, pp. 97–114.

Jonak J, Karpiński R, Siegmund M, Wójcik, A & Jonak, K 2020, 'Analysis of the rock failure cone size relative to the group effect from a triangular anchorage system', *Materials*, vol. 13, no. 20, pp. 4657.

Kaiser, PK & Cai, M 2012, 'Design of rock support system under rockburst condition', *Journal of Rock Mechanics and Geotechnical Engineering*, vol. 4, no. 3, pp. 215–227.

Kaiser, PK & Moss, A 2022, 'Deformation-based support design for highly stressed ground with a focus on rockburst damage mitigation', *Journal of Rock Mechanics and Geotechnical Engineering*, vol. 14, no. 1, pp. 50–66.

Kang, H, Wu, Y, Gao, F, Lin, J & Jiang, P 2013, 'Fracture characteristics in rock bolts in underground coal mine roadways', *International Journal of Rock Mechanics and Mining Sciences*, vol. 62, pp. 105–112.

Lhoste, E, Comte, F, Brown, K, Alain, D, David, J, Violaine, P, ... Cassandre, S L 2023, 'Bacterial, archaeal, and eukaryote diversity in planktonic and sessile communities inside an abandoned and flooded iron mine (Quebec, Canada)', *Applied Microbiology*, vol. 3, no. 1, pp. 45–63.

Li, CC 2010, 'Field observations of rock bolts in high stress rock masses', *Rock Mechanics and Rock Engineering*, vol. 43, no. 4, pp. 491–496.

Manafi, MS, Deng, A & Taheri, A 2022, 'Utilisation of extrusion method in geotechnical tests: conception and theoretical analysis', *Arabian Journal of Geosciences*, vol. 15, no. 5, pp. 449.

Markovic, M 2022, *Seismic Exploration Solutions for Deep-Targeting Metallic Mineral Deposits: From High-fold 2D to Sparse 3D, and Deep-learning Workflows*, PhD thesis, Uppsala University, Uppsala.

Mazaira, A & Konicek, P 2015, 'Intense rockburst impacts in deep underground construction and their prevention', *Canadian Geotechnical Journal*, vol. 52, no. 10, pp. 1426–1439.

Morrison, DM 1989, 'Rockburst research at Falconbridge's Strathcona mine, Sudbury, Canada', *Pure and Applied Geophysics*, vol. 129, pp. 619–645.

Ranjith, PG, Zhao, J, Ju, M, Radhika, VS, De, S, Tharaka, DR & Adheesha, KMSB 2017, 'Opportunities and challenges in deep mining: a brief review', *Engineering*, vol. 3, no. 4, pp. 546–551.

Saadat, M, Taheri, A & Kawamura, Y 2021, 'Incorporating asperity strength into rock joint constitutive model for approximating asperity damage: an insight from DEM modelling', *Engineering Fracture Mechanics*, vol. 248, pp. 107744.

Simser, BP 2019, 'Rockburst management in Canadian hard rock mines', *Journal of Rock Mechanics and Geotechnical Engineering*, vol. 11, no. 5, pp. 1036–1043.

Taheri, A & Tani, K 2010, 'Assessment of the stability of rock slopes by the slope stability rating classification system', *Rock Mechanics and Rock Engineering*, vol. 43, pp. 321–333.

Taheri, A, Royle, A, Yang, Z & Zhao, Y 2016a, 'Study on variations of peak strength of a sandstone during cyclic loading', *Geomechanics and Geophysics for Geo-Energy and Geo-Resources*, vol. 2, pp. 1–10.

Taheri, A, Yfantidis, N, Olivares, C, Connelly, B & Bastian, T 2016b, 'Experimental study on degradation of mechanical properties of sandstone under different cyclic loadings', *Geotechnical Testing Journal*, vol. 39, no. 4, pp. 673–687.

Verma, R K, Nguyen, G D, Karakus & Taheri, A 2021, 'Capturing snapback in indirect tensile testing using AUSBIT-Adelaide University Snap-Back Indirect Tensile test', *International Journal of Rock Mechanics and Mining Sciences*, vol. 147, pp. 104897.

Wang, Q, Jiang, Z, Jiang, B, Gao, H, Huang, Y & Zhang, P 2020, 'Research on an automatic roadway formation method in deep mining areas by roof cutting with high-strength bolt-grouting', *International Journal of Rock Mechanics and Mining Sciences*, vol. 128, pp. 104264.